Biogeophysical impacts of peatland forestation on regional climate change in Finland

Y. Gao[1,2], T. Markkanen[1], L. Backman[1], H. M. Henttonen[3], J.-P. Pietikäinen[1], H. Mäkelä[1], A. Laaksonen[1,4]

[1]{Finnish Meteorological Institute, P.O. Box 503, FI-00101 Helsinki, Finland}

[2]{University of Helsinki, Department of Physics, P.O. Box 64, FI-00014 Helsinki, Finland}

[3]{Finnish Forest Research Institute, P.O. Box 18, FI-01301 Vantaa, Finland}

[4]{University of Eastern Finland, Department of Applied Physics, P.O. Box 1627, FI-70211 Kuopio, Finland}

Correspondence to: Y. Gao (yao.gao@fmi.fi)

Abstract

Land cover change can impact climate by influencing surface energy and water balance. Unproductive peatlands were vastly drained to stimulate forest growth in Finland over the second half of 20th century. The aim of this study is to investigate the biophysical effects of peatland forestation on climate change in Finland. Two sets of 18-year climate simulations were done with the regional climate model REMO, using land cover data based on pre-drainage (1920s) and post-drainage (2000s) Finnish National Forest Inventories. Results show that in the most intensive peatland forestation area which located in the middle west of Finland, the differences in monthly averaged daily mean two meter air temperature show a spring warming of up to 0.43 K in April, whereas a slight cooling of less than 0.1 K in general, is found from May till October. Consequently, snow clearance day over that area is advanced up to 5 days in the mean of 15 years. No clear signal is found for precipitation. Through analyzing the simulated temperature and energy balance terms, as well as snow depth over five selected

subregions, a positive feedback induced by peatland forestation is found between decreased surface albedo and increased surface air temperature in the snow melting period. Our modelled results show good qualitative agreements with observational data. In general, decreased albedo in snow-melting period and increased evapotranspiration in the growing period are the most important biogeophysical aspects induced by peatland forestation that cause changes in climate.

1 Introduction

Climate response to anthropogenic land cover change happens more locally and occurs on a much shorter time scale, compared to global warming due to increased greenhouse gases (IPCC, 2013). The influences on climate from biogeophysical effects caused by land cover changes can enhance or reduce the projected climate change (Bathiany et al., 2010; Bonan, 2008; Feddema et al., 2005; Gálos et al., 2011; Göttel et al., 2008; Ge and Zou, 2013; Pielke et al., 2011; Pielke et al., 1998; Pitman, 2003). Especially for the climate impacts of past large-scale afforestation, studies show that the most obvious effect from the increase of forests in boreal areas is warming during snow-cover period due to decreased surface albedo and in tropical areas with sufficient soil moisture is cooling in summer time from increased evapotranspiration (ET) (Bala et al., 2007; Betts, 2000; Betts et al., 2007).

Vast areas of unproductive peatlands have been drained to grow forests for timber production in northern European countries (Päivänen and Hånell, 2012). In Finland, it is the dominant land cover change over the last half century, due to the high fraction of pristine peatland and the needs for timber production. The total peatland area of Finland was estimated to be 9.7 million ha in the 1950s (Ilvessalo, 1956). In the beginning of 2000s, the area of drained peatland for forestry was estimated to be 5.7 million ha by Minkkinen et al. (2002) and 5.5 million ha by Tomppo et al. (2011). The area of drained peatlands is unlikely to increase further because no more public subsidization are given for the first-time drainage of peatlands, along with the increased awareness of natural conservation (Metsätalouden kehittämiskeskus Tapio, 1997). The area of restored mires was 15 000 ha between 1990-2008 (www.biodiversity.fi/en/indicators/mires/mi17-mire-restoration) (Kaakinen and Salminen, 2006). However, land cover change is not only a result of human land use activities but can also be a consequence of climate change. Global warming in the future is also considered to be a factor that affects boreal peatland through water-level drawdown due to increased ET (Laiho et al., 2003; Laine et al., 1995).

Attention has been paid to the climate effects of peatland forestation. A decrease in the local night-time minimum temperature during the growing season was observed roughly for the first 15 years after drainage (Solantie, 1994). The reason for this nocturnal cooling phenomenon is the insulation of lower soil layers from the atmosphere by dry peat. Therefore, the heat flux from a drained peat soil cannot compensate the radiative cooling at the surface, which leads to a drop in daily minimum temperature (Venäläinen et al., 1999). On a longer time scale, the growing forest on formerly open peatlands leads to a decrease in albedo. The reasons for this are the darker tree-cover in comparison to the lighter grass-cover in snow free period, and the partial snow cover in forest areas compared to the full snow cover in open area in snow-cover period. This increases daily maximum temperature due to an increase in the absorption of short-wave radiation (Solantie, 1994). A consistent result was found by Lohila et al. (2010) based on radiation and albedo measurements at different drained and undrained peatland sites, as well as the observed long-term surface temperatures in Finland. In southern Finland (<65° N), the day-time maximum (night-time minimum) temperature in April has increased by 0.64 (0.37) K/decade during 1961 to 2008, along with about a total of 2.7 m[...] unproductive peatlands (Hökkä et al., 2002). This indicates an incre[...] temperature range in April due to a greater increase in day-time maxim[...] time minimum temperatures, which is possibly a result of the change in su[...] properties after drainage.

is this for peatlands or in general?

However, these studies related to peatland forestation are based on site-level data alone. The climate effects of peatland forestation have not been quantified on a regional scale/country level by investigating biogeophysical effects. Also, the magnitude and pattern of land use change effects on climate is quite dependent on regional conditions, for instance soil property, topography, and so on. Information from regional studies is essential for the development of future strategies on climate mitigation or forest management. Thus, it is necessary to investigate the effects regionally and systematically. In recent years, regional climate models have become suitable for simulating regional climate in a fine resolution to resolve small scale atmospheric circulation (Déqué et al., 2005; Jacob et al., 2007; Jacob et al., 2001; McGregor, 1997). For this, a regional climate model with realistic land scheme to interpret more detailed land surface information needs to be applied.

In this study, the long-term climate effects caused by peatland forestation are assessed from two sets of 15-year simulation results with the regional climate model REMO, by using the historical (1920s) and present-day (2000s) land cover conditions, respectively. The intention is to investigate the biogeophysical impacts of past peatland forestation on climate change in Finland.

2 Model description and methodology

2.1 REMO climate model

The regional climate model REMO is a three-dimensional hydrostatic atmospheric circulation model developed at Max Plank Institute, Germany (Jacob et al., 2007; Jacob and Podzun, 1997; Jacob et al., 2001). Its dynamical core is based on the 'Europamodell', the former numerical weather prediction model of German Weather Service (Majewski, 1991). The land surface scheme (LSS) of REMO mainly follows that of the global atmosphere circulation model ECHAM4 (Roeckner et al., 1996), with several physical packages updates (details will be shown later). The prognostic variables are: pressure, temperature, horizontal wind components, specific humidity, cloud liquid water and ice. REMO is driven by large scale forcing data according to the relaxation scheme (Davies, 1976). The eight outer most grid boxes at each lateral boundary are the sponge zone.

Because land cover is central for this study, a brief introduction of the LSS in REMO is given below. In REMO LSS, the total area of each model grid box is composed of fractions of land (vegetation cover and bare soil), water (ocean surface and inland lake) and sea ice (Semmler et al., 2004). The biogeophysical characteristics of major land cover classes (Olson, 1994a, b) are described by surface parameters: background surface albedo (albedo over snow-free land areas), roughness length, fractional green vegetation cover, leaf area index (LAI; one-sided green leaf area per unit ground area), forest ratio (fr; fractional coverage of trees regardless of their photosynthetic activity), soil water holding capacity (maximum amount of water that plants may extract from the soil before wilting begins) and vol[illegible] (percentage of moisture in a soil column below which pl[illegible] Hagemann et al., 1999). The land surface par[illegible]tional coverage of land cover types wit[illegible] length which is averaged logarithmi[illegible]9). As LAI, fractional green vegetation c[illegible]gly depend on the vegetation phenology, t[illegible]cycles by using a monthly varying growth factor which determines the growth characteristics of the vegetation (Hagemann, 2002; Rechid and Jacob, 2006). The growth factor for latitudes higher than 40 degrees North or South is derived from a two meter temperature climatology (Legates and Willmott, 1990), in other latitudes the fraction of photosynthetically active radiation is used.

This is unclear: do you consider the change of vegetation (e.g. forest growth) during the 18-year simulation? If this is the case the growth factor should be explained in a detailed manner.

The simple bucket scheme (Manabe, 1969) is used for soil hydrology where the partitioning of surface runoff and infiltration follows the Arno-Scheme (Dumenil and Todini, 1992). The soil temperature profile from the ground surface to around 10 m depth is described by five soil layers with increasing thickness. The heat conductivity and heat capacity, in the heat conduction equation for calculating the soil temperature, are dependent on the soil types (Kotlarski, 2007). The distribution of soil types is from FAO/UNESCO soil map of the world (FAO/UNESCO, 1971-1981; Kotlarski, 2007).

The Arno-Scheme used for the soil hydrology was further improved by considering the

This is a bit unclear: later om l. 170 - 174 you explain that CORINE land cover map is used.

high resolution subgrid-scale heter … climate model gridbox (Hagemann and Gates, 2 … heterogeneity is set to be 10 times higher than the re … standard REMO land cover map - Global Land Cover Characteristics Database (GLCCD) (Loveland et al., 2000; U.S. Geological Survey, 2001). The three parameters in the improved Arno-Scheme are accounting for the shape of the subgrid distribution of soil water capacities (Beta), subgrid minimum (W_{min}) and maximum (W_{max}) soil water capacity. Also, the original annual background albedo cycle was modified by using MODIS satellite data between 2001 and 2004 in order to derive more realistic global distributions of pure soil albedo and pure vegetation albedo, which are then used to compute the annual background albedo cycle with monthly varying LAI (Rechid, 2008; Rechid et al., 2009).

2.2 The model domain and land cover data sets

Our model domain covers Fennoscandia, a part of Russia and the northern part of Central Europe, and it is centred around Finland (Fig. 1). Typical features influencing climate of this domain include: the North Atlantic Ocean and the Baltic Sea that surround the Fennoscandian countries; many inland lakes located in Sweden and Finland; the relatively high Scandinavian mountain range, while the rest of the area is with topography lower th … level.

Earlier you say that there are 9.7 Mha peatlands

The default land c … GLCCD. However, its description of the land cover in Finland is … ance, there is no peatland in Finland in GLCCD, whereas 7.4% (22377 km2) of land is covered by unproductive peatland areas in the 10th Finnish National Forest Inventory (FNFI10) (Korhonen et al., 2013). GLCCD was therefore substituted by the more realistic and up to date CORINE land cover map (CLC; 2006) for the same model domain in Gao et al. (2014), except for the Russian part where CLC (2006) is not available. Unfortunately, land cover maps describing land cover conditions of Finland before the most intensive period of peatland drainage in 1960s are quite limited. Nevertheless, the data collected in the 1st Finnish National Forest Inventory (FNFI1) provides a possibility for tracing back the land cover condition of Finland in 1920s (Ilvessalo, 1927; Tomppo et al., 2010). The FNFI10 is adopted to describe the land cover condition of Finland in 2000s instead of CLC (2006), for the aim to avoid the uncertainties in compari[illegible]over classification methods and different sp[illegible]er maps are post-products that we[illegible]NFI field measurement data. The[illegible]NFI1 and FNFI10 land cover maps [illegible] maps are in 3 km resolution and include ten la[illegible]menclature.

So you mean in this paragraph that the spatial resolution (or the units are) is the same as in CLC but contents have been taken from FNFI?

Maybe this paragraph is a bit difficult to follow.

The fractional coverage for the ten land cover classes over the land area of Finland in 1920s and the changes from 1920s to 2000s based on the two FNFI land cover maps are shown as below (fractional coverage in 1920s; changes from 1920s to 2000s): Coniferous Forest (33.0%; 5.2%); Mixed Forest (13.5%; -5.7%); Broad-leaved Forest (4.7%; -0.8%); Artificial Areas (0.7%; 4.1%); Natural Grasslands (3.4%; -3.4%); Peat Bogs (14.3%; -5.2%); Open Spaces (1.5%; -0.1%); Transitional Woodland/Shrub (18.9%; 4.3%); Moors and heathland (2.1%; 0.7%); and Agricultural Areas (8.0%; 0.9%). Regional differences of those land cover classes can be seen in Fig. 2. In the FNFI maps, the land cover class Peat Bogs is defined as naturally treeless peatland and also pine mires where the stocking level is low or the mean height of trees is below 5 m at maturity. Therefore, the shifting from Peat Bogs to forests represents the major land cover change due to peatland forestation.

In addition to regional inspections, five subregions were selected to represent different land cover change conditions between FNFI1 and FNFI10. This was done to specifically assess the local climate effects of different intensities of peatland forestation (Fig.1; Table 1). From subregion1 [illegible]he reduction of Peat Bogs. Subregion1 and subr[illegible]in the middle and south of Finland, respe[illegible]decreases in the fractional coverage of Peat B[illegible]eases were mainly compensated by Coniferous Forest. The decrease in the fractional coverage of Peat Bogs was 2% less in subregion2 than that in subregion1, but the increase in the fractional coverage of Coniferous Forest was 5% higher in subregion2 than that in subregion1. The

This para is difficult to follow. I suggest presenting the information (percentages) as table.

total increase in the fractional coverage of forest types was about 16% in both subregion1 and subregion2. Subregion3 is located in the east of subregion1. There was 12% decrease in the fractional coverage of Peat Bogs, but instead of increase of forests, the fractional coverage of Transitional Woodland/Shrub increased by 14.3%. Subregion4 is an area where the most intensive anthropogenic activities have occurred in the five subregions. There was 14% decrease in the fractional coverage of forest types and 3.8% decrease in that of Peat Bogs, while 5.7% increase in the fractional coverage of Artificial Areas and 10.5% increase in that of Agriculture Areas. Subregion5 is an area with 8.64% increase in the fractional coverage of Peat Bogs and 16.3% decrease in the fractional coverage of forest types. Herein, one should notice that some uncertainties may arise from sampling in the FNFI1 and FNFI10 data. This goes especially for FNFI1, where the distance between inventory lines was as [illegible] subregions which are smaller than 100 km × 100 km may [illegible] actual land cover changes precisely. However, signals ave[illegible] not reflect the dynamics of the changes when diverse land cover changes are involved. Therefore, small subregions can be considered as hypothetical scenarios to represent different kinds of land cover changes and their local climate impacts.

I do not understand what you are trying to say here.

Moreover, the FNFI data only covers the land surface in Finland without considering inland lakes. Therefore, the land sea mask in the model domain is adopted from CLC (2006). In addition, the land cover conditions of the area outside Finland in the model domain are the same as those, i.e. based on CLC (2006) and GLCCD, in Gao et al. (2014) and thus identical in both simulations. Additionally, in order to allocate the surface parameters to appropriate land cover classes, the standard GLCCD land cover classes are related to the ten land cover classes in the FNFI maps through comparing the definitions of land cover classes (Table 2).

2.3 Modifications in REMO LSS in this study

Most of the surface parameters follow the built-in parameter values. However, large deviations were found when comparing the parameterized albedo with observed albedo. Moreover, the method for background albedo parameterization is not suitable for land use change studies because the vegetation albedo and the soil albedo maps are both derived from satellite albedo data which is measured in 2001-2004 with respect to land cover over that period. A new method, Land Use Character Shifts (LUCHS), has been proposed for land cover change studies (Preuschmann, 2012). It derives the annual background albedo cycle for certain land use types in one region from good quality remote sensing datasets – a surface albedo dataset and a land cover mask that are produced in the same time period. Unfortunately, LUCHS is not feasible for high latitude areas, where snow cover prevents the possibility of deriving background albedo values from satellite albedo data. Hence, a simplified method is developed in this study to derive the background albedo values of the ten land cover classes in FNFI land cover map. It is based on the assumption that the vegetation albedo map and the soil albedo map in current REMO LSS are feasible to describe the albedo values of the land cover condition in FNFI10, because the two datasets are overlapping in time. Therefore, the soil albedo and the vegetation albedo values, in model gridboxes that satisfy a requirement of 80% coverage of one land cover class in FNFI10, are averaged to represent the soil and vegetation albedo values of that land cover class. The 80% threshold was decreased to 50% for Natural Grasslands, Peat Bogs and Artificial Areas, as none of the model gridboxes have an 80% coverage of those land cover classes in Finland. The derived albedo values and the standard deviations for each land cover class in FNFI maps are shown in Table 3. The maximum background albedos, calculated based on the derived soil and vegetation albedo for FNFI land cover classes, are then compared with the summer time albedo of similar land cover classes for a southern (Hyytiälä; 61°51'N and 24°17'E) and a northern (Värriö; 67°48'N and 27°52'E) Finnish observation stations. The station values are estimated by a linear unmixing approach with the land use and forestry maps in combination with the MODIS BRDF/albedo product (Kuusinen et al., 2013). The derived and observed albedo values show good agreement for Peat Bogs, Mixed Forest, Transitional Woodland/Shrub and Agricultural Areas, as well as for Artificial Areas. Although the maximum albedo values of Coniferous Forest and Broad-leaved Forest in this study are roughly around 0.01 higher than those in Kuusinen et al. (2013), they are reasonable for considering albedo differences between land cover classes (Fig.3). The three land cover classes (Natural Grasslands, Moors and heathland, Open Spaces) are not found at the two stations, however they take up only small proportions in the FNFI land cover maps.

The snow albedo scheme for calculating the surface albedo during snow-cover period was also found to require some improvements. When there is snow on the ground, the surface albedo in REMO LSS is a function of background albedo, snow albedo and snow depth. The snow albedo depends linearly on snow surface temperature and fr (Kotlarski, 2007). Based on previous studies (K... 2007; Räisänen et al., 2014; Roesch et al., 2001), the a... in this study were increased ... In addition, the a_{min} (T=0°C) ... decreased to 0.25 (Fig. 4). The linear relationship with snow surface temperature and forest ratio is still adopted.

This relationship requires a better explanation: either from physical principles or reference to work, in which it was developed.

Moreover, the three parameters for describing the subgrid heterogeneity of soil hydrology (Hagemann and Gates, 2003), Beta, W_{min} and W... scale of 6 km resolution. It is 1/3 of the 18 km REMO r... that the spatial resolution of the FNFI land cover maps is ... compared to that of the default GLCCD land cover map.

Why this is the reason for 6 km resolution?

Corrections were also made to some of the surface parameters of Coniferous Forest and Mixed Forest, to obtain a better mutual consistency of the surface parameters for the three forest types. For Coniferous Forest, the fractional green vegetation cover in dormancy season and in growing seasons, and also the f... 0.8, respectively, as proposed for Fennoscandi... Forest, the fractional green vegetation cover an... be half of those parameters in the growing season.

Add some words about calculation of dynamics of snow cover. It is an important model component in relation to the main result.

3 Experiment design

Two simulations were conducted with the FNFI1 and FNFI10 land cover maps representing the land cover conditions before and after peatland forestation activities in

Finland, respectively. The simulations were driven with 6-hourly lateral boundary conditions from ECWMF ERA-Interim reanalysis data (Simmons et al., 2007) from 1 January 1979 to 31 December 1996. The 18-year forward runs were preceded with 10-year (1 August 1979 - 1 January 1990) simulations in order to stabilize the deep soil temperatures and soil moistures. The last 15-year (1 December 1981 - 30 November 1996) out of the 18-year forward simulations were adopted for further analysis. The analyzed period starts from December 1st in order to keep all the three winter months continuous. The simulated first one and a half years were excluded in order to minimize the influences of the initial boundary conditions on simulated climate conditions which are with much quicker adaptation speed than deep soil temperature. The model grid is in 18 km resolution horizontally and extends over 27 vertical levels (up to 25 km). The model time step was set to 90 s and the time steps of output variables are 6-hourly for 3D variables and hourly for 2D variables. Daily data covering 24 hours is processed from 1800 UTC of previous day to 1700 UTC of the current day. For 6-hourly data, 1800 UTC of the previous day and 0000 UTC, 0600 UTC, 1200 UTC of the current day were used for daily values. For this study domain, the growing season and the dormancy season cover the period from May to October and from November to April, respectively.

4 Results

The land cover change effects on regional climate conditions in Finland are analyzed based on the differences in climate variables between the post-drainage and pre-drainage simulations (FNFI10 – FNFI1). This 'delta change approach' is adopted to eliminate the uncertainties related to model bias (Gálos et al., 2011; Jacob et al., 2008).

4.1 Effects on climate over Finland

The differences in monthly averaged daily mean two meter air temperature (T_{2m}) are quite heterogeneous temporally and spatially (Fig. 5). The most noticeable difference in T_{2m}, up to 0.43 K, takes place in the most intensive peatland forestation area in the middle west of Finland in April. The warming is also evident in February and March, with differences of 0.2 K in this area. However, T_{2m} turns to show a slight cooling, generally less than 0.1 K, in a few parts of this area from May to October. There are also two regions in northern Finland that show opposite changes compared to the peatland forestation area in the middle west of Finland with cooling in spring and warming in the growing season. This is because of decreased forest cover and increased fraction of Peat Bogs in those two areas from FNFI1 to FNFI10 based land cover maps. An increase of less than 0.2 K is seen in T_{2m} in the southeast of Finland in July and August, as well as in the very south of Finland throughout the growing season, which are mainly due to the change from Mixed Forest to Coniferous Forest and the increased Artificial Areas, respectively. The 15-year averaged monthly precipitation only shows small differences, less than 10 mm/month, in varied patterns in the model domain from April to August (Fig. 6).

The snow clearance day is also an important indicator of spring-time climate change in high latitude areas (Peng et al., 2013). Therefore, the snow clearance day for each gridbox is determined for Finland over the 15 years. The snow clearance day is defined here as the first day after which the total number of snow covered days does not exceed the total number of snow free days, and the selection of this day ends before midsummer in a year. The differences between the 15-year averaged snow clearance days of the two simulations (Fig. 7) show almost the same pattern as the differences in T_{2m} in April (Fig.5). In the peatland forestation area in the middle west of Finland, the snow clearance days are mostly advanced from 0.5 to 3 days and in a few gridboxes advanced by up to 5 days in the 15-year mean. The two small areas in the north of Finland with reverse land cover changes in comparison to peatland forestation show up to two days delay in general. In the very south of Finland, the snow clearance days are also generally advanced in accordance with the warming seen in T_{2m}, but delayed in several scattered gridboxes, due to increased fraction of Artificial Areas at the expense of forests.

4.2 Effects on climate over five subregions

T_{2m} and precipitation, as well as several closely related climate variables (surface albedo, net surface solar radiation, snow depth, ET) for the five subregions were processed into 11-day running means to reduce the influence of day to day variations. The differences between the simulations in each regionally averaged climate variables were further averaged over the 15 years (Fig. 8). Herein, the date information (DOY, day of year) represents the middle contributing day of the 11-day averaging period.

T_{2m} of subregion1 shows a warming of 0.1 K to 0.2 K from February till the end of March, and an evident peak from early April to early May (DOY 95 to DOY 125) which reaches a maximum of 0.5 K in late April. T_{2m} of subregion2 has the same trend as subregion1 throughout the whole year, but the warming is much smaller and the biggest difference occurs in the beginning of April being only 0.12 K. This is consistent with the differences in snow depth. The decrease of snow depth in subregion1 is two to three times larger than that in subregion2, and the snow-cover period in subregion2 is shorter along with an earlier maximum difference in snow depth. Moreover, those characteristics of the differences in snow depths are in agreement with the differences in surface albedo because snow is the key factor that controls the surface albedo in snow-cover period. From the beginning of May to the beginning of October, T_{2m} turns to show a cooling of less than 0.1 K in subregion1 and subregion2, because the cooling caused by ET exceeds the warming caused by slightly lower albedo. The variability of the differences in net surface solar radiation in the growing season is induced by the variability of cloud cover rather than surface albedo. In November, December and January, the differences in T_{2m} vary in both directions. In high latitude areas, incoming solar radiation is quite small and cloud cover fraction is high in late autumn and winter. Therefore, the differences in surface albedo are not able to induce differences in net surface solar radiation in this period. Instead, the surface air temperature is sensitive to changes in long wave radiation balance that may lead to atmospheric air temperature inversion under clear sky, manifesting itself as extreme cold surface air temperature. Thus, the variability of the differences in cloud cover caused by short term variations in the climate contributes to varied differences in T_{2m} in this period.

The differences in T_{2m} for subregion3 show a warming of less than 0.1 K from DOY 91 to DOY 120, but also warming in an even smaller magnitude throughout the growing season. The difference in surface albedo in subregion3 is close to 0, although the difference in snow depth is similar to that of subregion2 but with a time lag of around 15 days in the most intensive point. In subregion4, the snow depth shows a quite small increase from the beginning of January till the end of March, which is consistent with the increase in surface albedo and explains the slight decrease of up to 0.1 K in T_{2m}, from middle of February till the end of March. Subregion5 performs opposite characteristics compared to subregion1 and subregion2 for all the investigated variables. The absolute differences in snow depth of subregion5 are smaller than those of subregion1, but larger than those of subregion2. Because subregion5 is located in the north of Finland, the biggest difference of snow depth occurs later than that of subregion1. The magnitude of the maximum differences in T_{2m} in snow-cover period of subregion5 also lies between that of subregion1 and subreigon2, and happens later than that of subregion1.

The differences of T_{2m} in the growing season depend on the surplus of energy balance terms, where ET manifests itself as latent heat flux. In general, the increase of ET amount in subregion2 is slightly higher than that in subregion1. As a consequence, the decrease of T_{2m} in subregion2 is slightly larger than that in subregion1 during the growing season when the albedo difference is quite small. The decreased ET and the slightly decreased surface albedo together result in a slight warming in growing season in the other subregions. The extents of warming in the other subregions follow the magnitudes of the decreased ET amounts because the differences in surface albedo are almost the same in the growing season.

Precipitation has higher variability than ET throughout the year in the five subregions. In general, the differences in precipitation are much larger in the growing season than in the dormancy season, when they are close to 0 mm/day. In the growing season, the increase in precipitation of subregion1 occurs during a longer period and has a larger magnitude than that of subregion2. There are slight increases in the precipitation in subregion3 and also in subregion4, whereas the precipitation of subregion5 shows a decreasing tendency in the growing season, with the biggest differences less than 0.2 mm/day.

Furthermore, the maximum and minimum differences of gridpoint-wise and regionally averaged 11-day running mean of T_{2m} over 15 years for subregion1 were investigated as complements for the regionally averaged 15-year mean differences of subregion1 (Fig. 9). T_{2m} shows a maximum difference in gridpoint-wise of nearly 2 K in snow-melting period over the 15 years, which is 1 K higher than the maximum difference in regionally averaged T_{2m} over the 15 years and four times as much as that in the 15-year mean of regionally averaged T_{2m}. The timings of the three kinds of maximum differences in spring deviate from each other from 3 to 10 days. The minimum differences show only a small deviation between the gridpoint-wise and regional mean values over the 15 years. During the snow-melting period, the minimum differences of regionally averaged T_{2m} is above 0, but not the gridpoint-wise T_{2m}. The spring time differences between regional mean and gridpoint-wise extremes elucidate that even within one subregion with homogenous characteristics related to peatland forestation, the spring warming of T_{2m} is temporally and spatially heterogeneous. This implies that local effects are more pronounced than the regional and temporal statistics can reveal. For the rest of the year, the differences between the maximum (minimum) of the gridpoint-wise and regionally averaged T_{2m} are small and of more regional nature. In the period between November and January, the large variations of maximum (minimum) T_{2m} are contributed by the inversion effects due to short term variations in the climate.

Additionally, for a more thorough understanding of the relationships between spring warming and albedo changes in [illegible] period due to peatland forestation, two correlation relationships [illegible] 15 years for subregion1 (Fig. 10).

Put this in caption of Fig. 10

One is between maxi[illegible]y (DOY) and maximum surface albedo difference day (D[illegible]nflection day of total albedo (that is, the day when surface albedo just finishes a fast decrease from its wintertime level, DOY) and snow clearance day (DOY). The maximum temperature difference days match with maximum albedo difference days in 6 years, and the rest of the years generally show a delayed maximum temperature difference day compared to the maximum albedo difference day, with a maximum deviation of 14 days. In general, the snow clearance day correlates well with the inflection point of surface albedo. For most years, the differences are less than 6 days, but three years show differences up to around 20 days. In those years, sporadic snowfall with a small accumulated snow depth cannot really introduce differences in total surface albedo over the subregion but influences the determination of snow clearance day.

5 Discussion

The differences in temperature and precipitation, as well as the closely related variables such as surface albedo, snow depth, net surface solar radiation and ET are examined in this study, to evaluate the peatland forestation effects through changes in biogeophysical characteristics. Surface albedo shows a decrease of up to 0.064 in peatland forestation areas during snow-cover period, and also a slight decrease in the growing season, whereas LAI, roughness length, fractional green vegetation cover, and forest ratio are increased throughout the year after peatland forestation. Those changes lead to an increase in spring-time T_{2m}, which occurs locally in accordance with the decrease in surface albedo. In the growing season, an increase in ET related to the increased LAI and fractional green vegetation cover leads to more energy consumed by latent heat flux than gained by slightly lower albedo. Additionally, higher roughness length can play a role by increasing turbulent mixing and consequently the magnitudes of turbulent fluxes. Thus, the scattered differences in precipitation in summer are contributed by more convective structures, while for the rest of the year the precipitation is basically controlled by large-scale meteorology. From the analysis of the results in the five subregions, the differences in the climate variables show that their magnitudes are dependent on the extent of land cover changes, while the timings of the extremes mostly depend on geographical locations (latitudes) that define the radiation balance through the seasonal cycle. Results also illustrate a positive feedback induced by peatland forestation between lower surface albedo and warmer T_{2m} in the snow-melting period. The warming caused by lower surface albedo in snow-cover period due to more forest leads to a quicker and earlier snow melting, meanwhile, surface albedo is reduced and consequently surface air temperature is increased. Additionally, the maximum difference in the gridpoint-wise 11-day running mean of T_{2m} in spring warming period over the 15 years reaches 2 K in subregion1, which is four times of the 15-year mean of the corresponding regionally averaged values. This illustrates that the spring warming effect from peatland forestation is highly heterogeneous spatially and temporally.

To examine the realism of the simulated surface air temperature differences due to peatland forestation, monthly temperature trends over 40 years (1959 - 1998) were calculated linearly based on monthly mean temperature maps over Finland, which were interpolated from observational data and in 10 km resolution (Aalto et al., 2013). The observation based temperature trends show around 0.1 K/decade stronger spring warming in the peatland fo

Do you mean that REMO predicts winter time temperatures with bias?

than surrounding areas in February, M

the simulated T_{2m}. However, while

March, the modelled difference in T_{2m} is largest in April. This is because of the cold temperature bias in the dormancy season in REMO simulations over this domain (Gao et al., 2014). The negative temperature differences in the simulations for the two areas in the north of Finland are mainly due

the FNFI based land cover maps. For example, the inf

m2 artificial lake located in northeast Lapland

in the observational maps but not in the

You could test this by a simulation, in which you make this kind of change for the whole subregion1 (or all regions).

I do not understand why this “Only around 20% …” constitutes an explanation for differences in max. differences - the 20% change is also in the observations. Could it be that there are factors involved in max. observed differences that your simulations do consider?

averaged over subregion1 (Fig.8)

s in net surface solar radiation

eas and closed forested areas in

except for the variations in the

ved net surface solar radiation in

DOY 70) and 80 W/m^2 (on DOY

5.5 W/m^2 occurs on DOY 107 in

r subregion1. Only around 20% of

ch probably explains the smaller

magni

s in the si

results. Thus, supposing peatland forestation would have occurred on the entire subregion1, the maximum difference in net surface solar radiation could be roughly estimated to be five times larger and reach 32.5

W/m^2. The timing of the maximum difference in simulated results agrees better with observational data for northern Finland because of the cold temperature bias in the dormancy season. The evolution of the differences in both simulated and observation based net surface solar radiation in spring can be divided into three phases: a slow increase, a quick increase and a quick drop. For the simulated net surface solar radiation, the slow increase occurs from the beginning of January until the end of March, and appears to be mostly induced by the differences in snow depth on land cover classes. The following quick increase occurs in a much shorter period in April, within around 10 to 20 days. The quick drop of the differences in net surface solar radiation follows the strong decrease of snow cover. The quick increase and quick drop are mainly attributed to snow melting, which is very sensitive to warmed air temperature.

There are a number of model uncertainties affecting the outcome of this work. Although the maximum background albedo values of FNFI land cover classes in this study are broadly consistent with the summer time albedo values derived specially for two observation stations in Finland in Kuusinen et al. (2013), the estimated albedo for land cover classes in high latitude areas show variations in a range of studies. The mean summer time albedo for Coniferous Forest is only 0.079 in Hollinger et al. (2010), while it is 0.119 in our study. We used a summer albedo for Broad-leaved Forest of 0.146, which is higher than the albedo values for Deciduous in Kuusinen et al. (2013) but still lower compared to 0.156 for aspen in Betts and Ball (1997) and 0.152 for deciduous in Hollinger et al. (2010). The cropland albedo is 0.189 in Hollinger et al. (2010) and it is much higher than the cropland albedo of 0.156 used in our study. In the middle boreal zone of Finland, the albedo of Peat Bogs and the albedo of forest are on average 0.145 and 0.115 in Solantie (1988), respectively. Thus, compared to those values, our lower albedo for Peat Bogs and higher albedo for forest (even only considering Coniferous Forest) may underestimate the warming effect contributed by more absorbed solar radiation. However, it is hard to say because higher temperature could enhance ET. Furthermore, even albedo values of same land cover class could be different in different parts of Finland. In Solantie (1988), the mean albedo of barren bogs in southern Finland and also of the concentric raised bogs in the middle of Finland is only 0.128. Also, recent studies show that forest albedo is influenced by stand density and understory in different sites (Bernier et al., 2011).

In winter time, the snow albedo scheme is much more important than the background albedo in determining the surface albedo for high latitude areas. The snow albedo scheme in REMO does not adequately represent the complex conditions over forests, with the linear dependence on snow surface temperature. Snow properties and canopy conditions, such as snow water content, grain size and snow pack thickness, as well as impurities on the snow surface, have strong influence on snow albedo (Wiscombe and Warren, 1980). Moreover, there is no vertical structure of forests in REMO where the process of snow intercepted by canopy is crucial (Roesch et al., 2001). The canopy of forests is also important in causing a night-time warming by shelter effect in areas with successful peatland forestation after about 15 years (Venäläinen et al., 1999).

Besides, the subgrid variability of soil saturation within a model gridbox is taken into account as 1/3 times of the model resolution in the simple bucket hydrology scheme in REMO LSS for this study, which is restricted by the 3 km resolution of the FNFI land cover maps. This can lead to underestimation of the surface runoff because the differences between the two surface parameters, W_{max} and W_{min} are smaller over the model domain compared to that with when using 10 times finer resolution to represent the subgrid hydrologic heterogeneity with GLCCD or CLC (2006). The influence on surface runoff could further effect on precipitation and ET through soil moisture, and also related to energy fluxes (Hagemann et al., 2013).

Furthermore, uncertainties can also arise from the FNFI land cover maps due to sampling and the translations between land cover classes in different land cover maps.

6 Summary

To get a clear picture of peatland forestation effects on climate in Finland is important for future forest management by not only considering economic aspects but also global warming mitigation. In this paper, we investigated the long-term biogeophysical effects of peatland forestation on near-surface climate conditions in Finland by using a historical (1920s) and a present-day (2000s) land use map based on Finnish National Forest Inventory data in a regional climate model REMO. The differences between the two simulations in surface air temperature and precipitation were examined. The results show that peatland forestation induces a spring warming effect and a slight cooling effect in the growing season, but a varied pattern with less than 10 mm/month differences in precipitation over Finland from April to September. The temperature response in spring in simulation results is well in line with that seen in observational maps. In the most intensive peatland forestation area in the middle west of Finland, the monthly averaged daily mean surface air temperature show a warming effect of around 0.2 K in February and March and reach 0.43 K in April, whereas a cooling effect of in general less than 0.1 K is found from May till October. Consequently, the snow clearance days in model gridboxes over that area are advanced up to 5 days in the mean of 15 years. Furthermore, a more detailed analysis was conducted on five subregions with decreased fractions of transformation from peatland to other land cover classes. 11-day running means of simulated temperature, surface albedo, net surface solar radiation and snow depth, as well as precipitation and ET were averaged over 15 years. Results show a positive feedback induced by peatland forestation between decreased surface albedo and increased surface air temperature in snow-melting period. Overall, decreased albedo in snow-melting period and increased ET in the growing period as a result of peatland forestation are the most important biogeophysical aspects that cause changes in surface air temperature. The extent of these climate effects depend on the intensity and geological locations of peatland forestation.

In the future, for the aim to get a more precise assessment of the biogeophysical impacts of peatland forestation on regional climate conditions, more accurate land cover maps and land surface parameters are essential. Also, a more robust land surface scheme could enhance the representation of interactions between land surface and climate.

Acknowledgement

The study was funded by Helsinki University Centre for Environment (HENVI). We are also grateful to Stefan Weiher from Brandenburg Technical University, Germany, and Stefan Hagemann from Max Planck Institute for Meteorology, Germany, for their valuable comments on this work.

Appendix A: Methods in deriving FNFI land cover maps

The sample of FNFI1 (1921-1924) consisted of inventory lines oriented from southwest to northeast at a distance of 26 km across most parts of the country. The total length of measured lines was 13348 km, and the total number of assessed land figures was 93922. In CLC-classification method, mean tree height and crown cover are two important criteria for classifying land use classes. However, because crown cover was not measured in FNFI1, the growing stock volume corresponding to crown cover thresholds were estimated using naturally regenerated forests and unditched pine mires in FNFI9 (1996-2003) and in FNFI10 (2004-2010), according to vegetation zone, site type, mean height, and dominant tree species. Afterwards, fractions of the ten land cover classes that were used in this study were derived for the FNFI1 sample in FNFI1 by considering land use class, estimated growing stock volume classes, mean height, vegetation zone, site type, and tree species composition.

For the interpolation, the FNFI1 sample lines were firstly split into slices with 1 km intervals in S-N direction. The fractions of the ten land cover classes in each slice on inventory line (1380m on average) were then used in calculating sample variograms. Those sample variograms are then fitted into a variogram model to derive kriging predictions using the R version 2.15.2 package `gstat` (Pebesma, 2004; R Core Team, 2012). The block kriging was carried out separately for the fraction of each of the ten land cover classes with isotropic exponential (or spherical) variogram model and a block size of 50 km x 50 km. A raster map in 3 km resolution was then produced for the coverage of the ten land cover classes.

In FNFI10, a systematic cluster sample (more details can be found at: http://www.metla.fi/ohjelma/vmi/vmi10-otanta-en.htm) of 69388 plots was measured (Korhonen et al., 2013). The distance between clusters of plots (10-14 plots/cluster) varied between 5 km (in southern Finland) and 11 km (in northern Finland). The classification of FNFI10 dataset was processed in a similar way to the FNFI1 data, with the exception that crown cover thresholds for classifying land use classes can be used directly in FNFI10 because it is assessed. To derive the 3 km by 3 km grid map, the cluster means of the proportions of the ten land cover classes were first calculated and then the same interpolation method was used as for FNFI1.

References

Aalto, J., Pirinen, P., Heikkinen, J., and Venäläinen, A.: Spatial interpolation of monthly climate data for Finland: comparing the performance of kriging and generalized additive models, Theor Appl Climatol, 112, 99-111, 2013.

Bala, G., Caldeira, K., Wickett, M., Phillips, T. J., Lobell, D. B., Delire, C., and Mirin, A.: Combined climate and carbon-cycle effects of large-scale deforestation, Proceedings of the National Academy of Sciences, 104, 6550-6555, 2007.

Bathiany, S., Claussen, M., Brovkin, V., Raddatz, T., and Gayler, V.: Combined biogeophysical and biogeochemical effects of large-scale forest cover changes in the MPI earth system model, Biogeosciences Discussions, 7, 2010.

Bernier, P. Y., Desjardins, R. L., Karimi-Zindashty, Y., Worth, D., Beaudoin, A., Luo, Y., and Wang, S.: Boreal lichen woodlands: A possible negative feedback to climate change in eastern North America, Agricultural and Forest Meteorology, 151, 521-528, 2011.

Betts, A. K. and Ball, J. H.: Albedo over the boreal forest, Journal of Geophysical Research: Atmospheres (1984–2012), 102, 28901-28909, 1997.

Betts, R. A.: Offset of the potential carbon sink from boreal forestation by decreases in surface albedo, Nature, 408, 187-190, 2000.

Betts, R. A., Falloon, P. D., Goldewijk, K. K., and Ramankutty, N.: Biogeophysical effects of land use on climate: Model simulations of radiative forcing and large-scale temperature change, Agricultural and Forest Meteorology, 142, 216-233, 2007.

Bonan, G. B.: Forests and Climate Change: Forcings, Feedbacks, and the Climate Benefits of Forests, Science, 320, 1444-1449, 2008.

Claussen, M., Lomann, U., Roeckner, E., and Schulzweida, U.: A global dataset of land surface parameters,, Max Planck Institute for Meterology, Hamburgh, 1994.

Déqué, M., Jones, R., Wild, M., Giorgi, F., Christensen, J., Hassell, D., Vidale, P., Rockel, B., Jacob, D., and Kjellström, E.: Global high resolution versus Limited Area Model climate change projections over Europe: quantifying confidence level from PRUDENCE results, Climate Dynamics, 25, 653-670, 2005.

Davies, H. C.: A laterul boundary formulation for multi-level prediction models, Quarterly Journal of the Royal Meteorological Society, 102, 405-418, 1976.

Dumenil, L. and Todini, E.: A rainfall-runoff scheme for use in the Hamburg climate model, Advances in Theoretical Hydrology, A Tribune to James Dooge, 1992. 129-157, 1992.

FAO/UNESCO: Soil map of the world,, UNESCO, Paris, 1971-1981.

Feddema, J. J., Oleson, K. W., Bonan, G. B., Mearns, L. O., Buja, L. E., Meehl, G. A., and Washington, W. M.: The Importance of Land-Cover Change in Simulating Future Climates, Science, 310, 1674-1678, 2005.

Gálos, B., Mátyás, C., and Jacob, D.: Regional characteristics of climate change altering effects of afforestation, Environmental Research Letters, 6, 044010, 2011.

Göttel, H., Alexander, J., Keup-Thiel, E., Rechid, D., Hagemann, S., Blome, T., Wolf, A., and Jacob, D.: Influence of changed vegetations fields on regional climate simulations in the Barents Sea Region, Climatic Change, 87, 35-50, 2008.

Gao, Y., Weiher, S., Tiina Markkanen, Pietikäinen, J.-P., Gregow, H., Henttonen, H. M., Jacob, D., and Laaksonen, A.: Implementation of the CORINE land use classification in the regional climate model REMO, Boreal environment research, accepted, 2014.

Ge, J. and Zou, C.: Impacts of woody plant encroachment on regional climate in the southern Great Plains of the United States, Journal of Geophysical Research: Atmospheres, 118, 9093-9104, 2013.

Hökkä, H., Kaunisto, S., Korhonen, K. T., Päivänen, J., Reinikainen, A., and Tomppo, E.: Suomen suometsät 1951–1994, 2002. 2002.

Hagemann, S.: An improved land surface parameter dataset for global and regional climate models,, Max Planck Institute for Meteorology, Hamburg, 2002.

Hagemann, S., Botzet, M., Dümeni, L., and Machenhauer, B.: Derivation of global GCM boundary conditions from 1 KM lnad use satellite data,, Max Planck Institute for Meteorology, Hamburg, Germany, 1999.

Hagemann, S. and Gates, L. D.: Improving a subgrid runoff parameterization scheme for climate models by the use of high resolution data derived from satellite observations, Climate Dynamics, 21, 349-359, 2003.

Hagemann, S., Loew, A., and Andersson, A.: Combined evaluation of MPI-ESM land surface water and energy fluxes, Journal of Advances in Modeling Earth Systems, 5, 259-286, 2013.

Hollinger, D. Y., Ollinger, S. V., Richardson, A. D., Meyers, T. P., Dail, D. B., Martin, M. E., Scott, N. A., Arkebauer, T. J., Baldocchi, D. D., Clark, K. L., Curtis, P. S., Davis, K. J., Desai, A. R., Dragoni, D., Goulden, M. L., Gu, L., Katul, G. G., Pallardy, S. G., Paw U, K. T., Schmid, H. P., Stoy, P. C., Suyker, A. E., and Verma, S. B.: Albedo estimates for land surface models and support for a new paradigm based on foliage nitrogen concentration, Global Change Biology, 16, 696-710, 2010.

Ilvessalo, Y.: Suomen metsät vuosina 1921-24 vuosiin 1951-53: kolmeen valtakunnan metsien inventointiin perustuva tutkimus (The forests of Finland from 1921-24 to 1951-53. A survey based on three national forest inventories), Communicationes Instituti Forestalis Fenniae 47(1): 1-277, 1956.

Ilvessalo, Y.: Suomen metsät. Tulokset vuosina 1921-1924 suoritetusta valtakunnan metsien arviomisesta (Summary in English: The forests of Finland. Results of the general survey of the forests of the country carried out during the years 1921-1924), Communicationes ex Instituto Quaestionum Forestalium Finlandiae 11, Valtioneuvoston kirjapaino, 1927.

IPCC: Climate change 2013: The physical science basis. Working group 1 contribution to the fifth assessment report of the intergovernmental panel on climate change,, Cambridge, United Kingdom and New York, NY, USA, 1535 pp., 2013.

Jacob, D., Bärring, L., Christensen, O. B., Christensen, J. H., de Castro, M., Déqué, M., Giorgi, F., Hagemann, S., Hirschi, M., and Jones, R.: An inter-comparison of regional climate models for Europe: model performance in present-day climate, Climatic Change, 81, 31-52, 2007.

Jacob, D., Kotova, L., Lorenz, P., Moseley, C., and Pfeifer, S.: Regional climate modeling activities in relation to the CLAVIER project, IdŰjárás, 112, 141-153, 2008.

Jacob, D. and Podzun, R.: Sensitivity studies with the regional climate model REMO, Meteorology and Atmospheric Physics, 63, 119-129, 1997.

Jacob, D., Van den Hurk, B., Andrae, U., Elgered, G., Fortelius, C., Graham, L., Jackson, S., Karstens, U., KoÈpken, C., and Lindau, R.: A comprehensive model inter-comparison study investigating the water budget during the BALTEX-PIDCAP period, Meteorology and Atmospheric Physics, 77, 19-43, 2001.

Køltzow, M.: The effect of a new snow and sea ice albedo scheme on regional climate model simulations, Journal of Geophysical Research: Atmospheres, 112, D07110, 2007.

Kaakinen, E. and Salminen, P.: Mire conservation and its short history in Finland, Finland–land of mires, 23, 229-238, 2006.

Korhonen, K. T., Ihalainen, A., Viiri, H., Heikkinen, J., Henttonen, H. M., Hotanen, J. P., Mäkelä, H., Nevalainen, S., and Pitkänen, J.: Suomen metsät 2004–2008 ja niiden kehitys 1921–2008 (The forests of Finland in 2004-2008 and their development from 1921 to 2008), Metsätieteen aikakauskirja B, 1, 2013.

Kotlarski, S.: A subgrid glacier parameterisation for use in regional climate modelling, Ph.D. Ph.D University of Hamburg, Max Planck Institute for Meterology, Hamburg, Germany, 2007.

Kuusinen, N., Tomppo, E., and Berninger, F.: Linear unmixing of MODIS albedo composites to infer subpixel land cover type albedos, International Journal of Applied Earth Observation and Geoinformation, 23, 324-333, 2013.

Laiho, R., Vasander, H., Penttilä, T., and Laine, J.: Dynamics of plant-mediated organic matter and nutrient cycling following water-level drawdown in boreal peatlands, Global Biogeochemical Cycles, 17, 1053, 2003.

Laine, J., Vasander, H., and Laiho, R.: Long-term effects of water level drawdown on the vegetation of drained pine mires in southern Finland, Journal of Applied Ecology, 32, 785-802, 1995.

Legates, D. R. and Willmott, C. J.: Mean seasonal and spatial variability in global surface air temperature, Theor Appl Climatol, 41, 11-21, 1990.

Lohila, A., Minkkinen, K., Laine, J., Savolainen, I., Tuovinen, J.-P., Korhonen, L., Laurila, T., Tietäväinen, H., and Laaksonen, A.: Forestation of boreal peatlands: Impacts of changing albedo and greenhouse gas fluxes on radiative forcing, Journal of Geophysical Research: Biogeosciences, 115, G04011, 2010.

Loveland, T. R., Reed, B. C., Brown, J. F., Ohlen, D. O., Zhu, Z., Yang, L., and Merchant, J. W.: Development of a global land cover characteristics database and IGBP DISCover from 1 km AVHRR data, International Journal of Remote Sensing, 21, 1303-1330, 2000.

Majewski, D.: The Europa-Modell of the Deutscher Wetterdienst. ECMWF Seminar on numerical methods in atmospheric models, 2, 147-191, 1991.

Manabe, S.: Climate and the ocean circulation 1: I. The atmospheric circulation and the hydrology of earth's surface, Monthly Weather Review, 97, 739-774, 1969.

McGregor, J.: Regional climate modelling, Meteorology and Atmospheric Physics, 63, 105-117, 1997.

Metsätalouden kehittämiskeskus Tapio: Metsätalouden säädökset (Forestry regulations), Helsinki, 1997.

Minkkinen, K., Korhonen, R., Savolainen, I., and Laine, J.: Carbon balance and radiative forcing of Finnish peatlands 1900–2100 – the impact of forestry drainage, Global Change Biology, 8, 785-799, 2002.

Olson, J. S.: Global ecosystem framework-definitions: USGS EROS Data Center Internal Report,, Sioux Falls, SD, 37 pp., 1994a.

Olson, J. S.: Global ecosystem framework-translation strategy: USGS EROS Data Center Internal Report,, Sioux Falls, SD, 39 pp., 1994b.

Päivänen, J. and Hånell, B.: Peatland Ecology and Forestry: A Sound Approach, Department of Forest Ecology, University of Helsinki, 2012.

Pebesma, E. J.: Multivariable geostatistics in S: the gstat package, Computers & Geosciences, 30, 683-691, 2004.

Peng, S., Piao, S., Ciais, P., Friedlingstein, P., Zhou, L., and Wang, T.: Change in snow phenology and its potential feedback to temperature in the Northern Hemisphere over the last three decades, Environmental Research Letters, 8, 014008, 2013.

Pielke, R. A., Pitman, A., Niyogi, D., Mahmood, R., McAlpine, C., Hossain, F., Goldewijk, K. K., Nair, U., Betts, R., Fall, S., Reichstein, M., Kabat, P., and de Noblet, N.: Land use/land cover changes and climate: modeling analysis and observational evidence, Wiley Interdisciplinary Reviews: Climate Change, 2, 828-850, 2011.

Pielke, R. A., Sr, Avissar, R., Raupach, M., Dolman, A. J., Zeng, X., and Denning, A. S.: Interactions between the atmosphere and terrestrial ecosystems: influence on weather and climate, Global Change Biology, 4, 461-475, 1998.

Pitman, A. J.: The evolution of, and revolution in, land surface schemes designed for climate models, International Journal of Climatology, 23, 479-510, 2003.

Preuschmann, S.: Regional surface albedo characteristics - analysis of albedo data and application to land-cover changes for a regional climate model, Ph.D. Ph.D., University of Hamburg, Max Planck Institute for Meterology, 2012.

R Core Team: R: A Language and Environment for Statistical Computing. R Foundation for Statistical Computing, Vienna, Austria, 2012,, ISBN 3-900051-07-0, 2012.

Räisänen, P., Luomaranta, A., Järvinen, H., Takala, M., Jylhä, K., Bulygina, O., Riihelä, A., Laaksonen, A., Koskinen, J., and Pulliainen, J.: Evaluation of North Eurasian snow-off dates in the ECHAM5. 4 atmospheric GCM, 2014. 2014.

Rechid, D.: On biogeophysical interactions between vegetation phenology and climate simulated over Europe, Ph.D. Ph.D., University of Hamburg, Max Planck Institute for Meterology, 2008.

Rechid, D. and Jacob, D.: Influence of monthly varying vegetation on the simulated climate in Europe, Meteorologische Zeitschrift, 15, 99-116, 2006.

Rechid, D., Raddatz, T., and Jacob, D.: Parameterization of snow-free land surface albedo as a function of vegetation phenology based on MODIS data and applied in climate modelling, Theor Appl Climatol, 95, 245-255, 2009.

Roeckner, E., Arpe, K., Bengtsson, L., Christoph, M., Claussen, M., Dümenil, L., Esch, M., Giogetta, M., Schlese, U., and Schultz-Weida, U.: The atmospheric general circulation model ECHAM4: Model description and simulation of the present-day climate, Max Planck Institute for Meterology, Hamburg, 1996.

Roesch, A., Wild, M., Gilgen, H., and Ohmura, A.: A new snow cover fraction parametrization for the ECHAM4 GCM, Climate Dynamics, 17, 933-946, 2001.

Semmler, T., Jacob, D., Schlünzen, K. H., and Podzun, R.: Influence of Sea Ice Treatment in a Regional Climate Model on Boundary Layer Values in the Fram Strait Region, Monthly Weather Review, 132, 985-999, 2004.

Simmons, A., Uppala, S., Dee, D., and Kobayashi, S.: ERA-Interim: New ECMWF reanalysis products from 1989 onwards, ECMWF newsletter, 110, 25-35, 2007.

Solantie, R.: Albedo in Finland on the basis of observations on aircraft,, Finnish Meterological Institute, Helsinki, 106 pp., 1988.

Solantie, R.: Suurten suo-ojitusten vaikutus ilman lämpötilaan erityisesti Alajärven Möksyn havaintojen perusteella (The impact of large scale wetland drainage on air tempearture based on observations in Möksy in Alajärvi),, Finnish Meterological Institute, Helsinki, 40 pp., 1994.

Tomppo, E., Gschwantner, M., Lawrence, M., and McRoberts, R. E.: National Forest Inventories, Pathways for Common Reporting. European Science Foundation, 2010. 2010.

Tomppo, E., Heikkinen, J., Henttonen, H. M., Ihalainen, A., Katila, M., Mäkelä, H., Tuomainen, H., and Vainikainen, N.: Designing and Conducting a Forest Inventory-case: 9th National Forest Inventory of Finland: Designing and Conducting a Forest Inventory-Case: 9Th National Forest Inventory of Finland, Springer, 2011.

U.S. Geological Survey: Global land cover characteristics data base version 2.0. U.S. Geological Survey, 2001.

Venäläinen, A., Rontu, L., and Solantie, R.: On the influence of peatland draining on local climate, Boreal environment research, 4, 89-100, 1999.

Wiscombe, W. J. and Warren, S. G.: A Model for the Spectral Albedo of Snow. I: Pure Snow, Journal of the Atmospheric Sciences, 37, 2712-2733, 1980.

Table 1. Changes of fractional coverage (%) of the ten land cover classes from 1920s to 2000s (FNFI10-FNFI1) in the five subregions.

Class	Legend	Subregion1	Subregion2	Subregion3	Subregion4	Subregion5
1	Coniferous Forest	13.40	18.03	-2.24	-11.74	-10.13
2	Mixed Forest	1.23	-3.46	-2.30	-1.86	-2.10
3	Broad-leaved Forest	1.24	0.98	1.68	-0.52	-4.11
4	Artificial Areas	4.44	4.95	2.44	5.69	2.52
5	Natural Grasslands	-4.41	-2.10	-1.71	-2.82	-1.60
6	Peat Bogs	-22.92	-20.82	-12.60	-3.80	8.64
7	Open Spaces	0.06	-0.12	-0.11	-0.31	-1.14
8	Transitional Woodland/Shrub	3.64	-0.72	14.26	4.84	9.12
9	Moors and heathland	0.00	0.00	0.00	0.00	-1.37
10	Agricultural Areas	3.31	3.26	0.57	10.52	0.17

Table 2. Translation between the ten land cover classes in FNFI maps and GLCCD land cover classes.

FNFI		GLCCD	
Class	Legend	Class	Legend
1	Coniferous Forest	21	Conifer Boreal Forest
2	Mixed Forest	23	Cool Mixed Forest
3	Broad-leaved Forest	25	Cool Broadleaf Forest
4	Artificial Areas	30	Cool Crops and Towns
5	Natural Grasslands	40	Cool Grasses and Shrubs
6	Peat Bogs	44	Mire, Bog, Fen
7	Open Spaces	53	Barren Tundra
8	Transitional Woodland/Shrub	62	Narrow Conifers
9	Moors and heathland	64	Heath Scrub
10	Agricultural Areas	93	Grass Crops

Table 3. Derived soil albedo and vegetation albedo values with standard deviations for the land cover classes in the FNFI maps, and the threshold used for each land cover class.

Class	Legend	Threshold (%)	Mean soil albedo ± SD	Mean vegetation albedo ± SD	Maximum albedo ± SD	Minimum albedo ± SD
1	Coniferous Forest	80	0.091 ± 0.017	0.121 ± 0.011	0.119 ± 0.012	0.119 ± 0.012
2	Mixed Forest	80	0.077 ± 0.003	0.134 ± 0.022	0.128 ± 0.020	0.119 ± 0.017
3	Broad-leaved Forest	80	0.091 ± 0.007	0.151 ± 0.001	0.146 ± 0.001	0.112 ± 0.005
4	Artificial Areas	50	0.090 ± 0.000	0.167 ± 0.000	0.145 ± 0.000	0.114 ± 0.000
5	Natural Grasslands	50	0.074 ± 0.000	0.211 ± 0.004	0.155 ± 0.002	0.077 ± 0.000
6	Peat Bogs	50	0.129 ± 0.054	0.133 ± 0.011	0.132 ± 0.023	0.129 ± 0.052
7	Open Spaces	80	0.147 ± 0.013	0.128 ± 0.001	0.136 ± 0.007	0.147 ± 0.013
8	Transitional Woodland/Shrub	80	0.074 ± 0.003	0.131 ± 0.008	0.120 ± 0.007	0.076 ± 0.004
9	Moors and heathland	80	0.124 ± 0.001	0.144 ± 0.001	0.142 ± 0.001	0.125 ± 0.001
10	Agricultural Areas	80	0.087 ± 0.011	0.184 ± 0.011	0.156 ± 0.011	0.128 ± 0.011

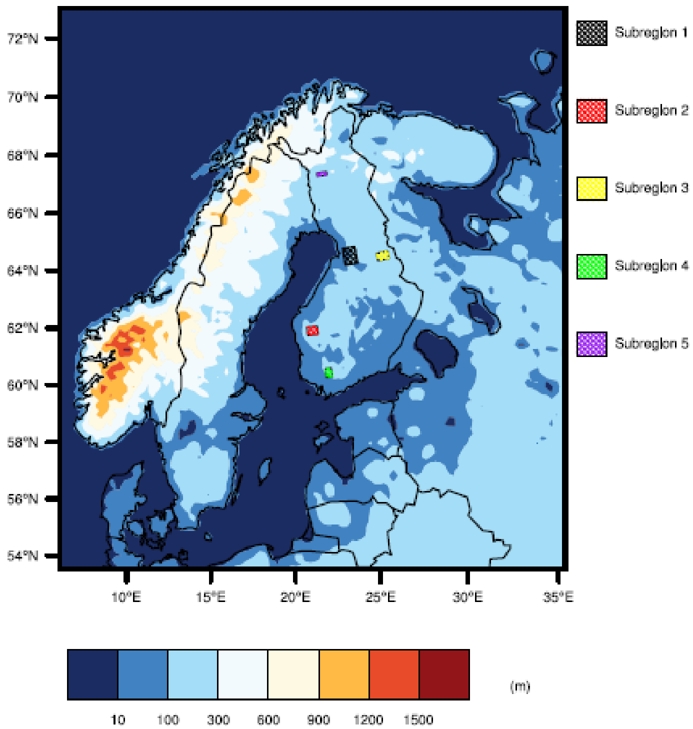

Figure 1. The model domain and the five selected subregions (the background is elevation in meters above sea level).

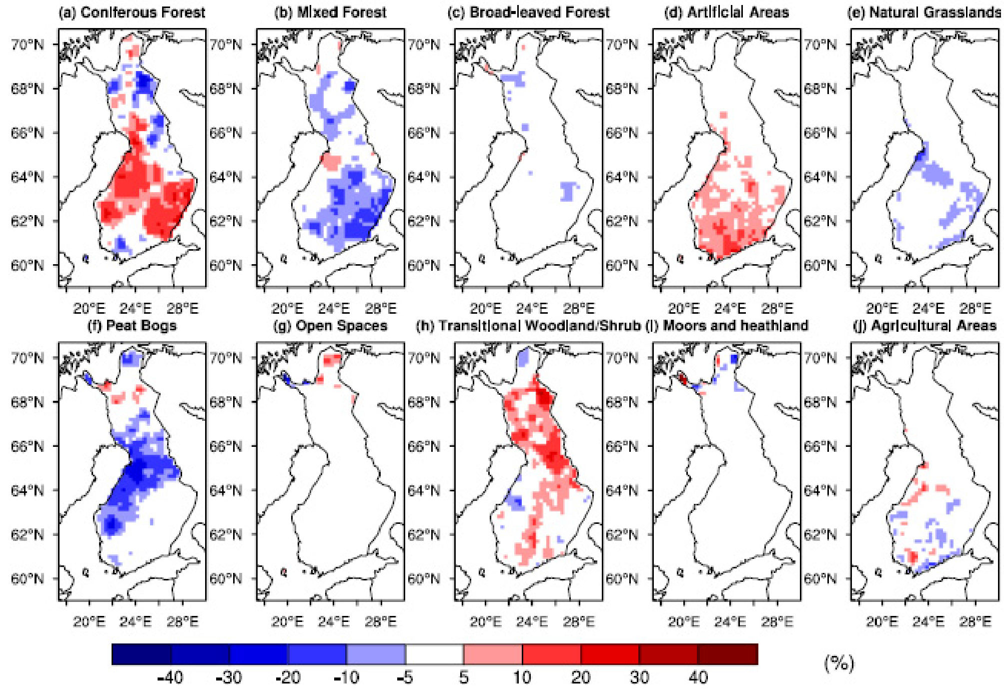

Figure 2. Changes of fractional coverage of the ten land cover classes in Finland from 1920s to 2000s (FNFI10-FNFI1).

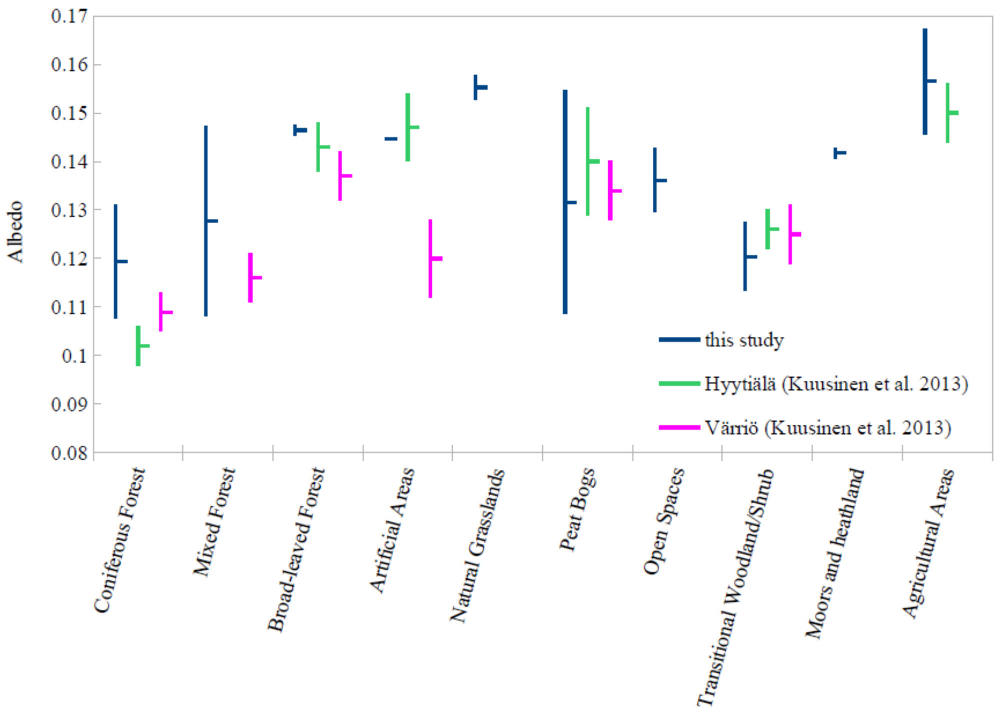

Figure 3. Comparison of the derived maximum background albedo values in a year (with the standard deviations) for the ten land cover classes in FNFI maps with the summer time albedo values (with the standard deviations) of the respective land cover classes observed at two Finnish stations in Kuusinen et al. (2013).

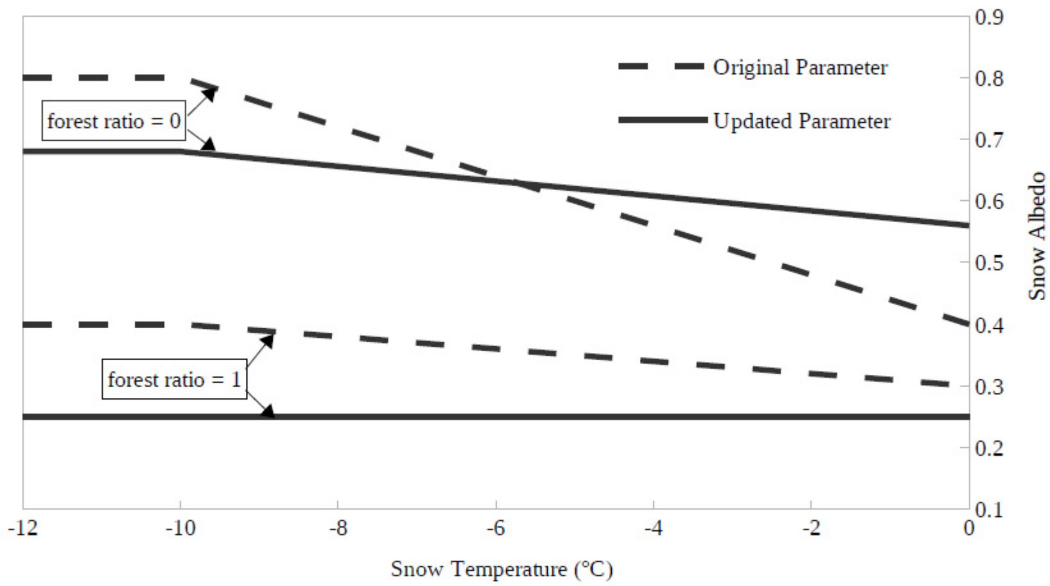

Figure 4. Modified snow albedo values in the snow albedo scheme (modified based on Fig. 3.6 in Kotlarski (2007)).

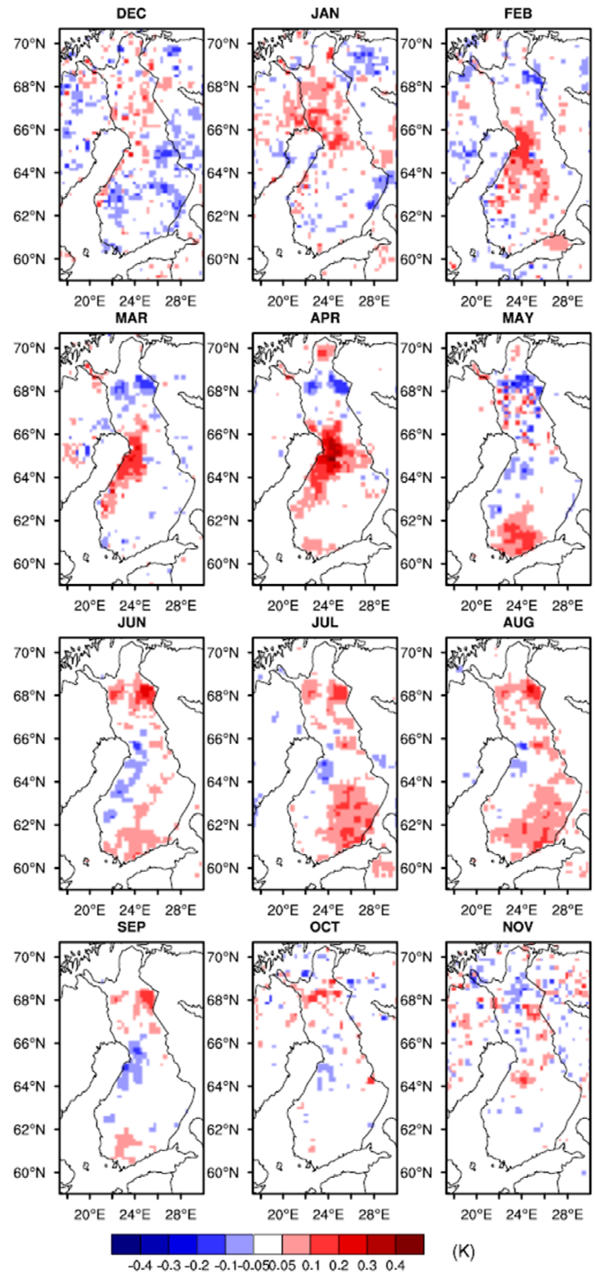

Figure 5. 15-year averaged differences (FNFI10 - FNFI1) in monthly averaged daily mean two meter air temperature.

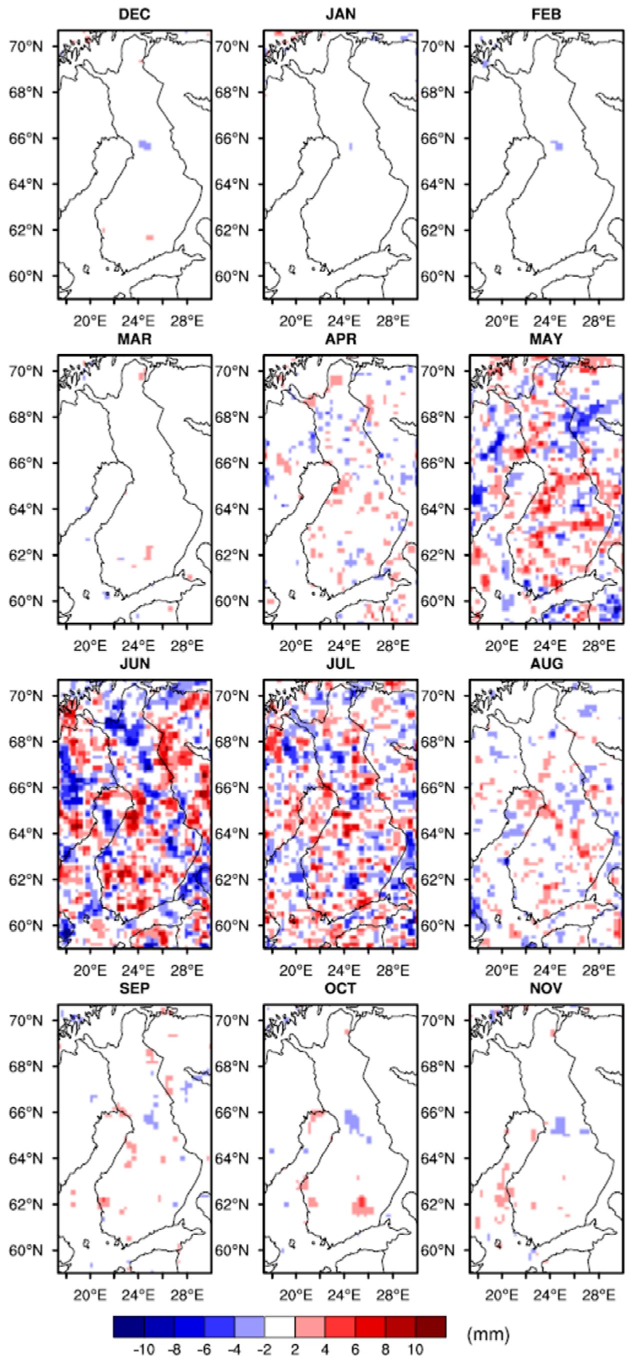

Figure 6. 15-year averaged differences (FNFI10 - FNFI1) in monthly precipitation.

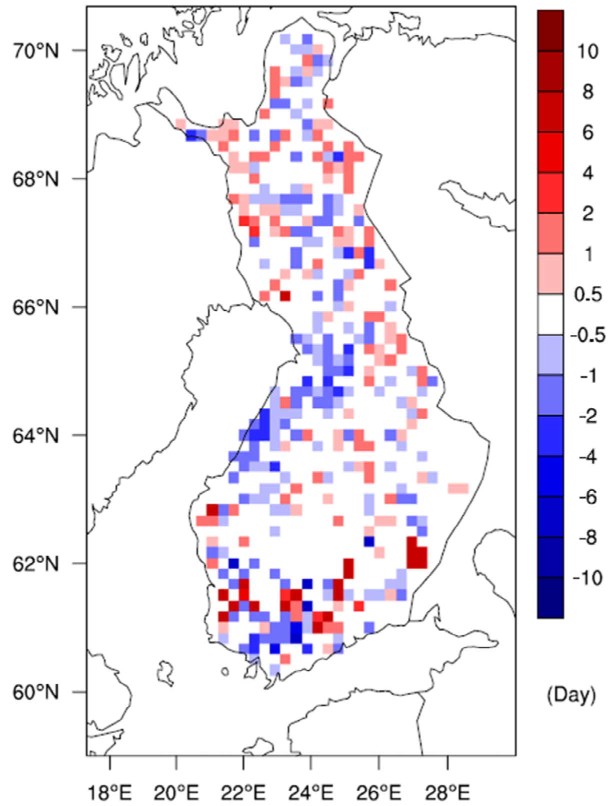

Figure 7. 15-year averaged differences (FNFI10 - FNFI1) in selected snow clearance days for model gridboxes.

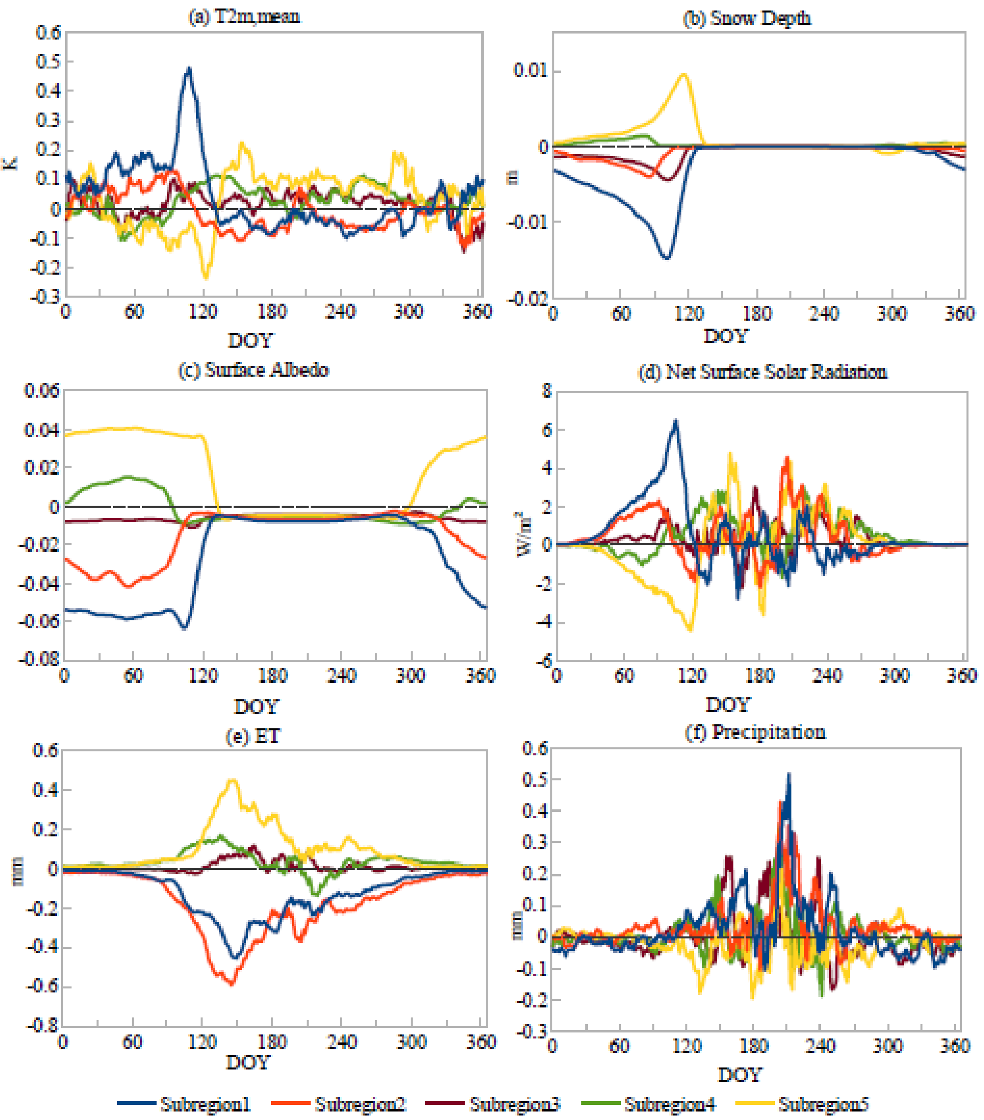

Figure 8. Regional mean differences in 11-day running mean of T_{2m}, surface albedo, net surface solar radiation, snow depth (presented as equivalent water), precipitation and ET averaged over 15 years for the five subregions. ET has the negative sign to represent more water loss, and vice versa.

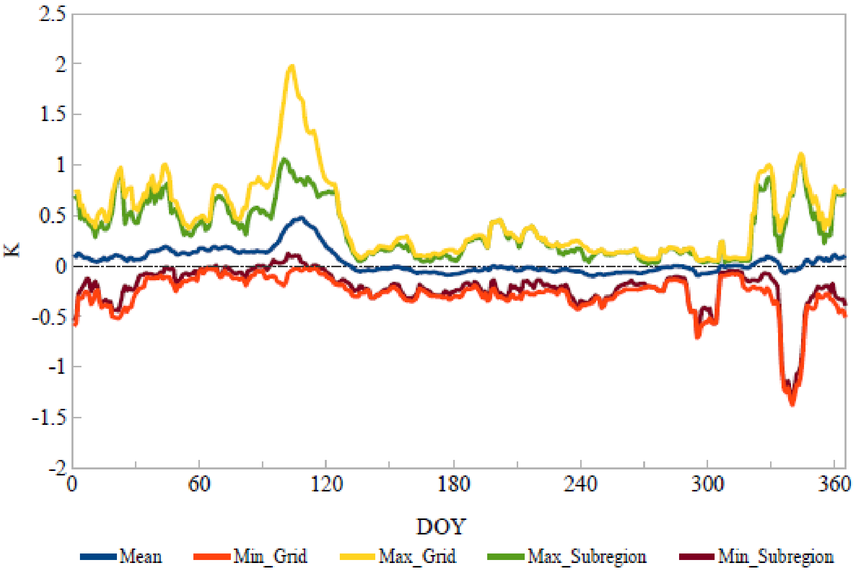

Figure 9. Maximum, minimum and mean differences of gridpoint-wise and regionally averaged 11-day running mean of T_{2m} over 15 years for subregion1.

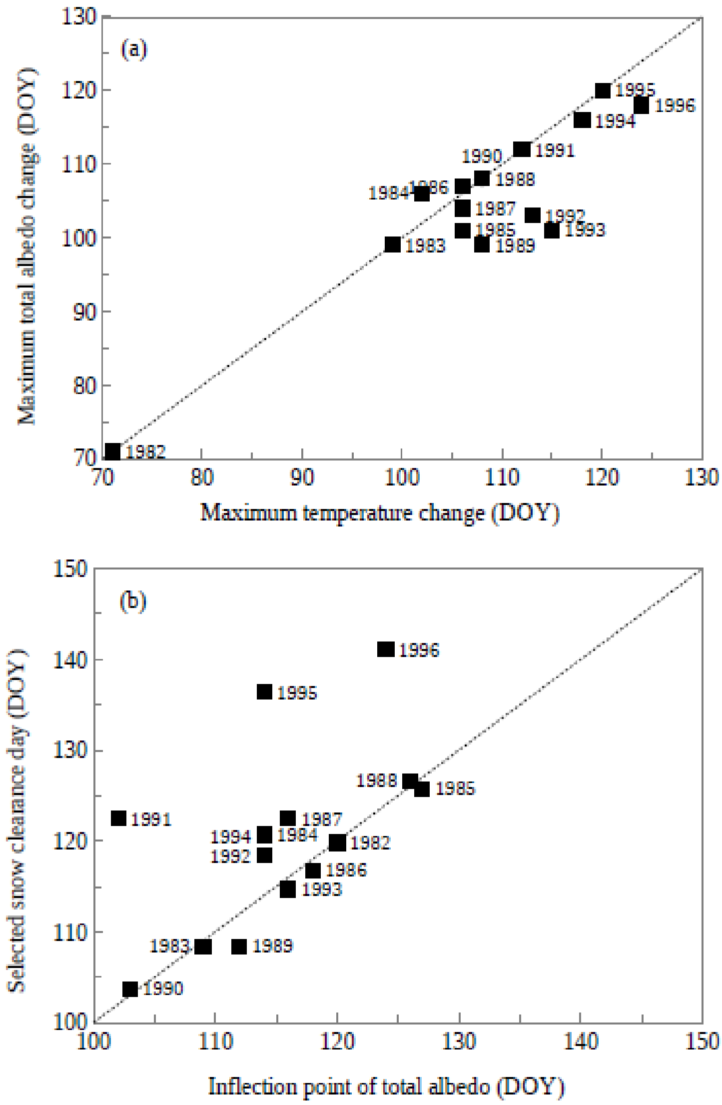

Figure 10. (a) Correlation between maximum temperature change day (DOY) and maximum total albedo change day (DOY). (b) Correlation between inflection day of total albedo (DOY) and selected snow clearance day (DOY). The plots show regional means over subregion1 for all the 15 years.

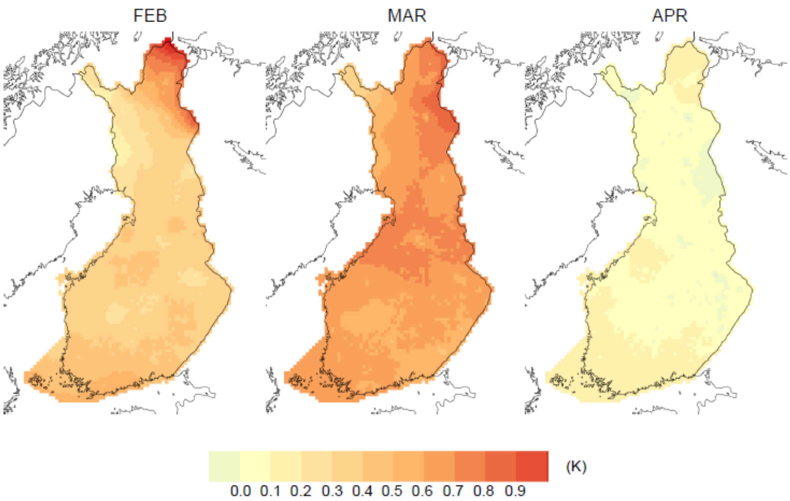

Figure 11. Surface temperature trends (K/decade) for February, March and April in Finland based on 40 years (1959-1998) observational data.